J|A|C|S
ARTICLES
Published on Web 01/31/2007

Characterization and Control of Lipid Layer Fluidity in Hybrid Bilayer Membranes

Neil A. Anderson, Lee J. Richter, John C. Stephenson, and Kimberly A. Briggman*

Contribution from the Department of Physics, National Institute of Standards and Technology, 100 Bureau Drive MS8443, Gaithersburg, Maryland 20899-8443

Received September 12, 2006; E-mail: kbriggma@nist.gov

Abstract: The main gel-to-liquid-crystal (LC) phase transition temperature, T_m, of the distal lipid layer in hybrid bilayer membranes (HBMs) under water was investigated using vibrational sum frequency spectroscopy (VSFS). VSFS has unique sensitivity to order/disorder transitions in the lipid acyl chains and can determine T_m for the lipid monolayers in HBMs. We recently reported the observation that T_m is raised and the transition width is broadened for the overlying phospholipid monolayer in HBM systems formed on densely packed crystalline self-assembled monolayers (SAMs) as compared to that of vesicles in solution. In this report, we establish that T_m for the lipid layer of HBMs can be controlled by proper choice of the SAM underlayer. The SAM underlayer of the HBM was systematically altered by using an alkane thiol, a saturated thiolipid, a mixed SAM of a saturated lipid−pyridine disulfide, and finally a mixed SAM of an unsaturated lipid−pyridine disulfide. T_m was measured for two different chain length saturated phosphatidylcholine lipid overlayers on these SAMs. The values obtained show that T_m of the lipid layer of HBMs is sensitive to the composition and/or packing density of molecules in the underlying SAM.

Introduction

The use of supported lipid membranes as research tools for developing novel biosensors and for interrogating the structure and function of membrane associated proteins is a topic of much scientific interest.[1−6] Supported bilayer membranes promise the ability to preserve a natural environment for amphipathic and hydrophobic proteins while providing a suitable platform for the application of interface-sensitive analytical techniques. Supported planar bilayers (SPBs) formed on glass,[7−9] mica,[10−12] or polymer[13−15] substrates have been suggested to mimic natural membranes by incorporating a hydration layer between the bilayer and substrate. However, these membrane mimics are often fragile (the bilayer is not well supported by the substrate[7]), and the hydration layer is not always thick enough to prevent an incorporated protein from coming in contact with the substrate.[16] Additionally, recent experiments have shown that some substrates (mica) affect the fluidity or phase behavior of lipids in the SPB.[10,11] As alternatives to SPBs, rigid tethers within a bilayer[17−19] (where one end of the tether is covalently linked to the solid substrate and the other is solvated in the applied lipid bilayer) have been incorporated, and hybrid bilayer membranes[20,21] (HBMs) (where one-half of the bilayer is a hydrophobic self-assembled monolayer (SAM) onto which a single lipid monolayer is applied) have been developed. These latter two approaches increase the stability and robustness of the bilayer system over long time periods. These systems are also generally easy to form through self-assembly methods, can cover large surface areas, and have been characterized by a variety of surface science techniques. The natural asymmetry of HBMs offers the additional ability to tailor each layer independently. Moreover, HBMs assembled on metals have been demonstrated for use in electrical biosensors.[4]

Many applications of HBMs, such as platforms for membrane protein structural or mechanistic studies, require full characterization of the physical properties of the HBM. For instance, the fluidity or phase state of both the lipid layer and the underlying SAM must be known and tailored to the application. We have recently reported measurements of the main gel-to-liquid-crystal (LC) phase transition temperatures (T_m) for a series of saturated phosphatidylcholine lipids (PCs) over perdeuterated

(1) Terrettaz, S.; Ulrich, W. P.; Vogel, H.; Hong, Q.; Dover, L. G.; Lakey, J. H. *Protein Sci.* **2002**, *11*, 1917−1925.
(2) McConnell, H. M.; Watts, T. H.; Weis, R. M.; Brian, A. A. *Biochim. Biophys. Acta* **1986**, *864*, 95−106.
(3) Sackmann, E. *Science* **1996**, *271*, 43−48.
(4) Cornell, B. A.; Braach-Maksvytis, V. L. B.; King, L. G.; Osman, P. D. J.; Raguse, B.; Wieczorek, L.; Pace, R. J. *Nature* **1997**, *387*, 580−583.
(5) Seifert, K.; Fendler, K.; Bamberg, E. *Biophys. J.* **1993**, *64*, 384−391.
(6) Tien, H. T. *Adv. Mater.* **1990**, *2*, 316−318.
(7) Tamm, L. K.; McConnell, H. M. *Biophys. J.* **1985**, *47*, 105−113.
(8) Rädler, J.; Strey, H.; Sackmann, E. *Langmuir* **1995**, *11*, 4539−4548.
(9) Hetzer, M.; Heinz, S.; Grage, S.; Bayerl, T. M. *Langmuir* **1998**, *14*, 982−984.
(10) Yang, J.; Appleyard, J. *J. Phys. Chem. B* **2000**, *104*, 8097−8100.
(11) Feng, Z. V.; Spurlin, T. A.; Gewirth, A. A. *Biophys. J.* **2005**, *88*, 2154−2164.
(12) Charrier, A.; Thibaudau, F. *Biophys. J.* **2005**, *89*, 1094−1101.
(13) Naumann, C. A.; Prucker, P.; Lehmann, T.; Rühe, J.; Knoll, W.; Frank, C. W. *Biomacromolecules* **2002**, *3*, 27−35.
(14) Baumgart, T.; Offenhausser, A. *Langmuir* **2003**, *19*, 1730−1737.
(15) Tanaka, M.; Sackmann, E. *Nature* **2005**, *437*, 656−663.
(16) Koenig, B. W.; Krueger, S.; Orts, W. J.; Majkrzak, C. F.; Berk, N. F.; Silverton, J. V.; Gawrisch, K. *Langmuir* **1996**, *12*, 1343−1350.
(17) Boden, N.; Bushby, R. J.; Clarkson, S.; Evans, S. D.; Knowles, P. F.; Marsh, A. *Tetrahedron* **1997**, *53*, 10939−10952.
(18) Raguse, B.; Braach-Maksvytis, V.; Cornell, B. A.; King, L. G.; Osman, P. D. J.; Pace, R. J.; Wieczorek, L. *Langmuir* **1998**, *14*, 648−659.
(19) Lahiri, J.; Kalal, P.; Frutos, A. G.; Jonas, S. J.; Schaeffler, R. *Langmuir* **2000**, *16*, 7805−7810.
(20) Plant, A. L. *Langmuir* **1993**, *9*, 2764−2767.
(21) Plant, A. *Langmuir* **1999**, *15*, 5128−5135.

10.1021/ja066588c CCC: $37.00

octadecanethiolate (dODT) SAMs.[22] These HBMs have a lipid phase transition temperature that is consistently ~10 °C above the phase transition temperature for the same lipids in vesicles in solution. That is, the lipid layer in HBMs remains crystalline well above the lipid bilayer melting temperature of vesicles. In cell membranes, the lipid bilayer is naturally maintained in the fluid (LC) state, and lipid composition and membrane fluidity are of crucial importance to biological activity.[23−27] Recognizing that the crystallinity of the underlying SAM is indeed a problem for the HBM systems, some groups have developed thiol-derivatized lipids to use as the SAM layer, so the SAM might better mimic a lipid membrane.[28,29] More sophisticated thiolated lipids have also been designed to provide a hydration layer between the SAM and the substrate through ethylene oxide[30−32] or peptide[33] spacer units incorporated between the thiol group and the lipid in the SAM. While HBMs with these molecules have been made and characterized by a variety of methods, there have not been any studies to date of how changing the underlying SAM chemistry influences the fluidity of the lipid layer.

The focus of this work is to study the fluidity of the upper lipid layer of an HBM while systematically introducing disorder into the underlying SAM. We use vibrational sum frequency spectroscopy (VSFS) to determine the gel-to-LC T_m for the lipid overlayer in an HBM and to characterize the phase state of the underlying SAM. In this Article, we report changes in T_m for two saturated phosphatidylcholine lipid overlayers as the underlying SAM chemistry is varied from an alkanethiol to a saturated thiolipid to a mixed SAM of a saturated lipid−pyridine disulfide to a mixed SAM of an unsaturated lipid−pyridine disulfide. At the phase transition temperature, melting of the acyl chains in the lipid overlayer causes a transformation from an essentially all-trans conformation to an acyl chain geometry incorporating many gauche defects. As a consequence, the VSFS spectrum changes dramatically. We are particularly interested in characterizing the phase behavior of HBMs to assess their utility for the incorporation and study of membrane spanning proteins. Our results show that changes in the composition of the underlying SAM in the HBM allow T_m for the lipid overlayer to be tuned by ~15 °C with respect to the phase transition temperature of the same lipid in vesicles.

Experimental Section

Certain equipment, instruments, or materials are identified in this paper in order to adequately specify the experimental details. Such identification does not imply recommendation by the National Institute of Standards and Technology nor does it imply the materials are necessarily the best available for the purpose.

Vibrational Sum Frequency Spectroscopy (VSFS). VSFS is an *in situ* technique that offers both interface specificity and submonolayer sensitivity. It has the usual strengths of vibrational spectroscopies shared by Raman scattering and infrared (IR) absorption spectroscopy. Additionally, because VSFS is symmetry forbidden in systems that are locally centrosymmetric, VSFS is particularly sensitive to order/disorder changes that characterize melting of lipid acyl chains. The theory of VSFS has been described previously.[34] Briefly, VSFS combines two incoming laser beams, one in the infrared (IR) at ω_{IR} and the other in the visible (VIS) at ω_{VIS}, at an interface or surface to produce a third beam at the sum frequency (SF), $\omega_{SF} = \omega_{IR} + \omega_{VIS}$. When ω_{IR} overlaps a SF active vibrational resonance of a molecule at the surface, the intensity of light generated at ω_{SF} is modulated. The intensity of the VSFS signal as a function of the infrared frequency may be modeled as:

$$I_{VSFS}(\omega_{IR}) \propto \left|B + \sum_q \frac{A_q \cdot e^{i\phi_q}}{\omega_{IR} - \omega_q + i\Gamma_q}\right|^2 \quad (1)$$

The first term, B, is the non-resonant contribution to the second-order nonlinear susceptibility, $\chi^{(2)}$, generated at the gold substrate. The second term represents a sum of the resonant contributions to $\chi^{(2)}$ from the different active vibrational modes, q, of molecules at the interface. These are modeled by Lorentzian line shapes, which adequately describe the data. Each mode has an amplitude, A_q, a center frequency ω_q, and a line width, Γ_q. For this paper, all VSFS spectra were acquired in the $p_{SF}p_{VIS}p_{IR}$ polarization combination, so the phase, ϕ_q, between the resonant and non-resonant contributions can vary with each resonant mode. Our particular experimental implementation of VSFS (broadband VSFS)[35] and its application to the study of SAMs[36] and HBMs[22,37] has been described previously. Specific to this work, the pulse energies and beam diameters were 3.5 μJ and 200 μm for the IR beam and 10 μJ and 400 μm for the VIS beam. The spectral resolution, determined by the picosecond narrow bandwidth VIS laser beam, was 6 cm^{-1}.

Traditionally, HBMs have consisted of an alkanethiolate SAM underlayer and a lipid overlayer.[21] To simplify the spectroscopy, we used fully protonated SAM underlayers and lipids with perdeuterated acyl chains. The VSFS data for deuterated acyl lipid chains were fit to six peaks determined from previous studies of a related system, perdeuterated octadecyl disulfide (dODDS) SAMs on Au.[36] The gel-phase frequencies and assignments for the C−D vibrational modes are: CD_3 (r^+) at 2067 cm^{-1}, CD_2 (d^+) at 2095 cm^{-1}, CD_3 (FR) at 2124 cm^{-1}, A1 at 2140 cm^{-1}, CD_2 (d^-) at 2204 cm^{-1}, and CD_3 (r^-) at 2218 cm^{-1}, as labeled in Figure 1. The ratio of the intensities of the CD_2 symmetric stretch (d^+) to the CD_3 symmetric stretch (r^+) was used for analysis of the degree of order/disorder of the deuterated lipid chains. For easier quantification, in the nonlinear least-squares fitting of the data to eq 1, the widths of the d^+ and r^+ modes were held constant at 12 and 7 cm^{-1}, respectively, and the frequencies were only allowed to vary ±3 cm^{-1} so the amplitudes could be ratioed directly. The nature of the A1 feature, clearly present in the SFG spectra of perdeuterated alkane chains, is uncertain; it can possibly be assigned to a Fermi resonance of the CD_2 d^+ mode. The specific assignment of the A1 feature is not essential to the analysis.

Chemicals and Materials. The lipids, 1,2-dimyristoyl-D54-*sn*-glycero-3-phosphocholine (d54-DMPC), 1,2-dipalmitoyl-D62-*sn*-glycero-3-phosphocholine (d62-DPPC), 1,2-dipalmitoyl-*sn*-glycero-3-phos-

(22) Anderson, N. A.; Richter, L. J.; Stephenson, J. C.; Briggman, K. A. *Langmuir* **2006**, *22*, 8333−8336.
(23) Strittmatter, P.; Rogers, M. J. *Proc. Natl. Acad. Sci. U.S.A.* **1975**, *72*, 2658−2661.
(24) Anderle, G.; Mendelsohn, R. *Biochemistry* **1986**, *25*, 2174−2179.
(25) Prenner, E. J.; Lewis, R. N. A. H.; Kondejewski, L. H.; Hodges, R. S.; McElhaney, R. N. *Biochim. Biophys. Acta* **1999**, *1417*, 211−223.
(26) Valiyaveetil, F.; Zhor, Y.; MacKinnon, R. *Biochemistry* **2002**, *41*, 10771−10777.
(27) Brian, A. A.; McConnell, H. M. *Proc. Natl. Acad. Sci. U.S.A.* **1984**, *81*, 6159−6163.
(28) Lingler, S.; Rubinstein, I.; Knoll, W.; Offenhäusser, A. *Langmuir* **1997**, *13*, 7085−7091.
(29) Krysinski, P.; Zebrowska, A.; Michota, A.; Bukowska, J.; Becucci, L.; Moncelli, M. R. *Langmuir* **2001**, *17*, 3852−3857.
(30) Lang, H.; Duschl, C.; Grätzel, M.; Vogel, H. *Thin Solid Films* **1992**, *210−211*, 818−821.
(31) Lang, H.; Duschl, C.; Vogel, H. *Langmuir* **1994**, *10*, 197−210.
(32) Steinem, C.; Janshoff, A.; Von dem Bruch, K.; Reihs, K.; Goossens, J.; Galla, H. J. *Bioelectrochem. Bioenerg.* **1998**, *45*, 17−26.
(33) Naumann, R.; Jonczyk, A.; Kopp, R.; Van Esch, J.; Ringsdorf, H.; Knoll, W.; Gräber, P. *Angew. Chem., Int. Ed. Engl.* **1995**, *34*, 2056−2058.
(34) Shen, Y. R. *Surf. Sci.* **1994**, *299−300*, 551−562.
(35) Richter, L. J.; Petralli-Mallow, T. P.; Stephenson, J. C. *Opt. Lett.* **1998**, *23*, 1594−1596.
(36) Yang, C. S. C.; Richter, L. J.; Stephenson, J. C.; Briggman, K. A. *Langmuir* **2002**, *18*, 7549−7556.
(37) Petralli Mallow, T. P.; Briggman, K. A.; Richter, L. J.; Stephenson, J. C.; Plant, A. L. *Proc. SPIE-Int. Soc. Opt. Eng.* **1999**, *3858*, 25−31.

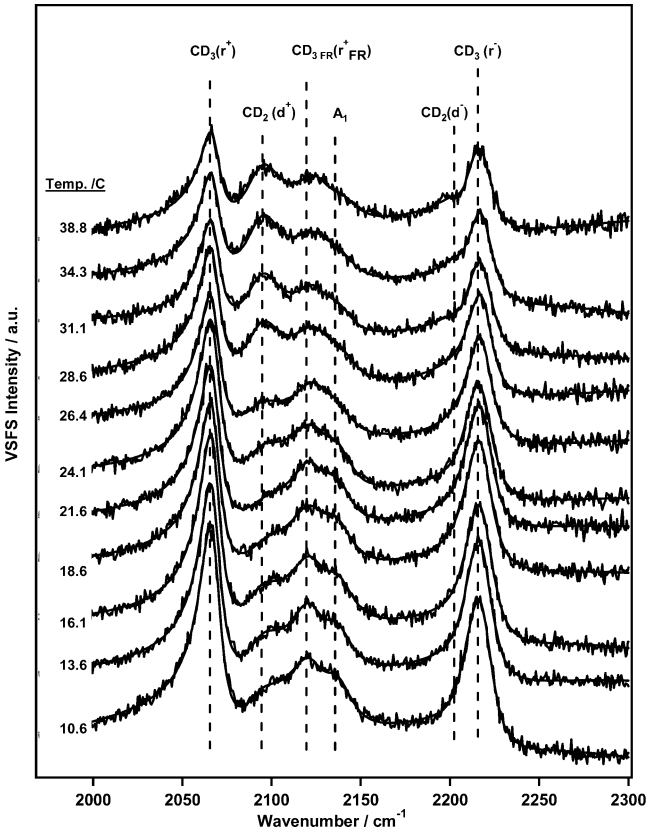

Figure 1. VSFS spectra and assignments of the C−D stretch region for an HBM of d54-DMPC/ODT as a function of temperature. Spectra are offset for clarity.

phothioethanol (DPPSH), 1,2-dipalmitoyl-*sn*-glycero-3-phosphoethanolamine-*N*-[3-(2-pyridyldithio)propionate] (DPPSSPyr), and 1,2-dioleoyl-*sn*-glycero-3-phosphoethanolamine-*N*-[3-(2-pyridyldithio)propionate] (DOPSSPyr), were obtained from Avanti Polar Lipids (Alabaster, AL) as lyophilized powders (>99%). Histological grade 2-propanol and octadecanethiol (ODT) were purchased from Sigma Aldrich Co. (St. Louis, MO). The 2-propanol was dried over molecular sieves before use. Ultrapure, deionized water was obtained from a Nanopure Diamond Life Science water purification system from Barnstead International (Dubuque, IA). Phosphate buffered saline (PBS; 1X without calcium chloride and without magnesium chloride) solution was obtained from Invitrogen Corp. (Carlsbad, CA). Deuterium oxide, D_2O (99.9%), was obtained from Cambridge Isotope Laboratories, Inc. (Andover, MA). Ethanol (200 proof) was used as received from Warner Graham, Inc. (Cockeysville, MD). Titanium (5 nm) and gold (250 nm) coating of the substrate slides was performed by Platypus Technologies, LLC (Madison, WI).

The sample cell was derived from a FCS2 microscopy chamber from Bioptechs (Butler, PA). A 15 μm Teflon spacer was sandwiched between a 2 mm calcium fluoride entrance window and a gold-coated microaqueduct slide inside the chamber. The gold-coated glass microaqueduct slide was made with two pairs of T-shaped grooves roughly 10 mm long that allow laminar flow in two isolated 20 mm wide channels across the sample. A peristaltic pump was used to push solution through the cell at a flow rate of about 1 mL·min^{-1}. The nominal volume of the flow cell was 3 μL. The IR and visible beams were co-incident on the calcium fluoride window at 67° and 45°, respectively. Because of refraction, the incident angles were nominally 45° and 33° at the solution/Au interface. Only aqueous solution was present in one channel, and lipid vesicles were introduced in the second. The first channel provided a reference spectrum for the second, significantly improving the low frequency noise in the baseline of the broadband VSFS measurement. All VSFS spectra shown were acquired with the samples under aqueous (H_2O or D_2O) solution. For phase transition studies, the temperature of the brass cell was controlled to within 0.1 °C by flowing thermostated water through the brass cell. With each increase in temperature, the cell was allowed to stabilize for 5 min before data acquisition began. The temperature was measured with a calibrated chromel−alumel thermocouple with a precision of ±0.1 °C and absolute accuracy of ±0.5 °C in contact with the back of the glass microaqueduct slide.

Table 1. Summary of Phase Transition Temperatures for d54-DMPC and d62-DPPC Lipid Outerlayers of HBMs[a]

overlayer	underlayer	T_m (°C)	transition width (°C)
d54-DMPC	ODT	26.9 ± 2.4	8.2 ± 3.9
d54-DMPC	DPPSH	34.4 ± 2.4	17.0 ± 3.9
d54-DMPC	DPPSSPyr	31.3 ± 2.4	13.6 ± 3.9
d54-DMPC	DOPSSPyr	18.3 ± 2.4	8.9 ± 3.9
unsupported d54-DMPC vesicles[b]		19.7 ± 0.2	2.0 ± 1.0
d62-DPPC	ODT	49.3 ± 2.4	13.3 ± 3.9
d62-DPPC	DPPSH	48.5 ± 2.4	12.5 ± 3.9
d62-DPPC	DPPSSPyr	37.7 ± 2.4	9.5 ± 3.9
d62-DPPC	DOPSSPyr	37.1 ± 2.4	7.6 ± 3.9
unsupported d62-DPPC vesicles[b]		36.4 ± 0.2	0.9 ± 0.3

[a] The quoted uncertainty is one standard deviation based on the pooled variance over a total of 19 measurements with 11 degrees of freedom. [b] Vesicles are 100 nm in diameter. See Chemicals and Materials.

Following the work in refs 38 and 39, we used Raman and IR spectroscopies to determine that T_m is 19.7 ± 0.2 and 36.4 ± 0.2 °C for 100 nm vesicles of d54-DMPC and d62-DPPC lipids reported in Table 1, respectively. The 100 nm vesicles were made by vesicle extrusion using an Avanti Polar Lipids Mini-Extruder (Alabaster, AL). Vesicles passed through a 100 nm polycarbonate membrane at least 15 times, and the vesicle diameter was determined by photon correlation spectroscopy using a Beckman Coulter N4 particle size analyzer (Fullerton, CA). Our measurement of the nominally 100 nm vesicles was 99 ± 11 nm. T_m is reported to be independent of size for vesicles of 70 nm diameter or larger.[40,41] The measured T_m for vesicles is consistent with the literature[42] and the general observation that T_m for perdeuterated PC lipids is slightly lower than that of analogous hydrogenated lipids.

HBM Preparation. HBMs were formed on the gold-coated glass microaqueduct slides, which were first cleaned in a UV ozone oven, rinsed with ultrapure water, and recleaned in the UV ozone oven. The cleaned gold surface was immediately immersed in to a 200 μM ethanolic solution of either ODT, DPPSH, DPPSSPyr, or DOPSSPyr for at least 14 h. The quality of the SAM films was verified by infrared reflection-adsorption spectroscopy (IRAS), VSFS, and ellipsometry. The gold slide was assembled with the Teflon spacer and CaF_2 window and mounted in a brass variable-temperature cell. The top lipid layer of the HBM was deposited by flowing lipid vesicles of either d54-DMPC or d62-DPPC in H_2O or PBS buffer through one of the laminar flow channels. Vesicles of d54-DMPC and d62-DPPC lipids were formed by the injection method.[43] Briefly, 1.5 mg (2 μmol) of phospholipid was weighed out, dissolved in 20 μL of dry 2-propanol, and injected with a pipet tip into 1 mL of vortexing ultrapure H_2O or PBS. The resulting solution was diluted by 10 to produce a concentration of 200 μM. As reported previously, the vesicles spontaneously fuse to the SAM, forming the lipid overlayer of the HBM.[37]

(38) Castresana, J.; Valpuesta, J. M.; Arrondo, J. L. R.; Goni, F. M. *Biochim. Biophys. Acta* **1991**, *1065*, 29−34.
(39) Devlin, M. T.; Levin, I. W. *J. Raman Spectrosc.* **1990**, *21*, 441−451.
(40) Koynova, R.; Caffery, M. *Biochim. Biophys. Acta* **1998**, *1376*, 91−145.
(41) Kennedy, A.; Hmel, P. J.; Seelbaugh, J.; Quiles, J. G.; Hicks, R.; Reid, T. J. *J. Liposome Res.* **2002**, *12*, 221−237.
(42) Guard-Friar, D.; Chen, C. H.; Englet, A. S. *J. Phys. Chem.* **1985**, *89*, 1810−1813.
(43) Silin, V. I.; Wieder, H.; Woodward, J. T.; Valincius, G.; Offenhausser, A.; Plant, A. L. *J. Am. Chem. Soc.* **2002**, *124*, 14676−14683.

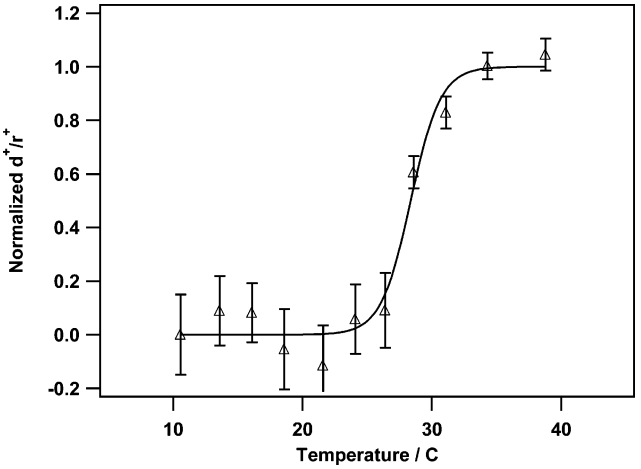

Figure 2. Normalized ratio of the d^+/r^+ amplitudes extracted from the fits to VSFS spectra of the d54-DMPC/ODT HBM from Figure 1 as a function of *T*. Also shown is a sigmoid fit to the d^+/r^+ ratio.

Results and Discussion

Figure 1 shows the VSFS spectra and assignments of the C−D stretches for the lipid acyl chains of a d54-DMPC/ODT HBM taken under water as a function of temperature, *T*. For $T < T_m$, d54-DMPC is in its gel phase, and its alkane chains have a crystalline, nearly all-trans configuration. In VSFS, this conformation results in near cancellation of signal from the ordered alternating methylene (CD_2) groups. However, above the melting temperature, $T > T_m$, the chains become disordered and gauche defects form, which break the centrosymmetry of the acyl chains and allow CD_2 modes to appear in the spectra. This is also accompanied by a loss of intensity of the CD_3 modes as the acyl chains become more disordered. It is well accepted that vibrational transitions associated with the lipidic acyl chains reflect order/disorder of chains in both linear[44,45] and nonlinear[46,47] spectroscopies. In related protonated systems, we previously showed the d^+/r^+ ratio can be used to determine T_m.[22] In Figure 1, the CD_3 r^+ feature is observed at 2067 cm^{-1}, and the CD_2 d^+ feature is at 2095 cm^{-1}. The lines through the data in Figure 1 are quantitative nonlinear-least-squares fits to eq 1. Figure 2 shows the ratio of the normalized d^+/r^+ amplitudes extracted from the fits as a function of *T*. At T_m, the d^+/r^+ ratio increases suddenly. Spectroscopic changes with *T* near T_m of lipid bilayers or multilayers are typically fit to a sigmoid[41,48] function, $S(T) = C + A/(1 + \exp((T - T_m)/D))$, where *C* is a constant, *A* is the amplitude, *T* is the temperature, T_m is the midpoint of the phase transition, and *D* is a width factor related to enthalpy of the phase transition and the average number of lipids in a domain. The theoretical basis for the sigmoid dependence has been previously discussed.[48] *S* may be the amplitudes or frequencies of spectral features that are different in the two phases. In the VSFS measurements, *S* is the d^+/r^+ ratio. Figure 2 also shows a fit of the d^+/r^+ ratio data to the sigmoid expression, which gives a value of $T_m = 28.3 \pm 0.7$ °C for d54-DMPC on ODT. This value of T_m is 8.6 °C greater than the value $T_m = 19.7 \pm 0.2$ °C for d54-DMPC vesicles. This experiment was also performed for an HBM of d62-DPPC on ODT. For this system, the value of T_m is 49.3 ± 0.6 °C, which is 12.9 °C greater than the value $T_m = 36.4 \pm 0.2$ °C for d62-DPPC vesicles. This increase in T_m for HBMs is consistent with previous findings of similar chain length protonated lipids on dODT.[22]

To explore the parameters important in producing an elevated T_m in HBMs, a series of SAMs were formed to systematically incorporate increased disorder into the underlayer. This was accomplished both by using mixed SAMs (to possibly space the molecules apart) and by employing molecules in their disordered state within the SAMs. In addition to ODT, the following molecules were used for the SAM: DPPSH, the acyl chain equivalent of a DPPC lipid but with the choline headgroup substituted by a thioethanol group; DPPSSPyr, also the acyl chain equivalent of a DPPC lipid, but the headgroup contains an amide linkage to a pyridine disulfide group; and DOPSSPyr, the acyl chain equivalent of DOPC (containing a 9-cis double bond in each chain), but with the choline headgroup substituted by an amide linkage to a pyridine disulfide group. These particular molecules were chosen because of their ability to self-assemble, their different degrees of disorder, and their commercial availability in high purity. The structures of these molecules are presented in Figure 3. Disulfides have been shown to readily form SAMs of equivalent structure to thiols by breaking the disulfide bond, thus forming two thiolate bonds to gold per molecule.[49] The naïve expectation is that DPPSSPyr and DOPSSPyr form mixed SAMs consisting of equimolar ratios of the lipid thiolate and the pyridine thiolate on the gold surface. This expectation is supported by IRAS measurements, confirming the presence of pyridine thiolate in the spectra of the DPPSSPyr SAM, with an absorption intensity equal to 50% of a pure pyridine thiolate monolayer.

SAMs of the molecules presented in Figure 3 were first characterized by VSFS under D_2O in the C−H stretch region (data not shown). For the ODT, DPPSH, and DPPSSPyr SAMs, the alkane chains remained well ordered at all temperatures $T < 65$ °C, that is, at all temperatures used in these experiments. For the DOPSSPyr SAM, the alkane chains have a 9-cis double bond in each acyl chain and the VSFS spectra have the signature of lipid chain disorder (i.e., the presence of CH_2 bands from gauche defects) at all temperatures. VSFS spectra of HBMs made of these SAMs with a deuterated lipid over layer of d62-DPPC in contact with D_2O were acquired at 23 °C in the C−H stretch region and are shown in Figure 4. The lack of a strong CH_2 symmetric stretch at 2845 cm^{-1} and the presence of a strong CH_3 symmetric stretch at 2873 cm^{-1} for the ODT, DPPSH, and DPPSSPyr based HBMs indicate that the hydrocarbon chains in the SAMs are in an all-trans configuration and crystalline, while the prominent CH_2 modes in the spectrum of the DOPSSPyr HBM indicate that the SAM acyl chains are disordered, by analogy to previously interpreted spectra.[22]

HBMs with both d62-DPPC and d54-DMPC as the lipid overlayers were formed on the SAMs characterized above. VSFS data were taken in the C−D stretch region and fit to eq 1. Representative plots resulting from sigmoid fits to the

(44) Spiker, R. C.; Levin, I. W. *Biochim. Biophys. Acta* **1976**, *455*, 560−575.
(45) Mantsch, H. H.; McElhaney, R. N. *Chem. Phys. Lipids* **1991**, *57*, 213−226.
(46) Roke, S.; Schins, J.; Muller, M.; Bonn, M. *Phys. Rev. Lett.* **2003**, *90*, 1281011−1281014.
(47) Gurau, M. C.; Castellana, E. T.; Albertorio, F.; Kataoka, S.; Lim, S. M.; Yang, R. D.; Cremer, P. S. *J. Am. Chem. Soc.* **2003**, *125*, 11166−11167.
(48) Kirchoff, W. H.; Levin, I. W. *J. Res. Natl. Bur. Stand. (U.S.)* **1987**, *92*, 113−128.
(49) Biebuyck, H. A.; Bain, C. D.; Whitesides, G. M. *Langmuir* **1994**, *10*, 1825−1831.

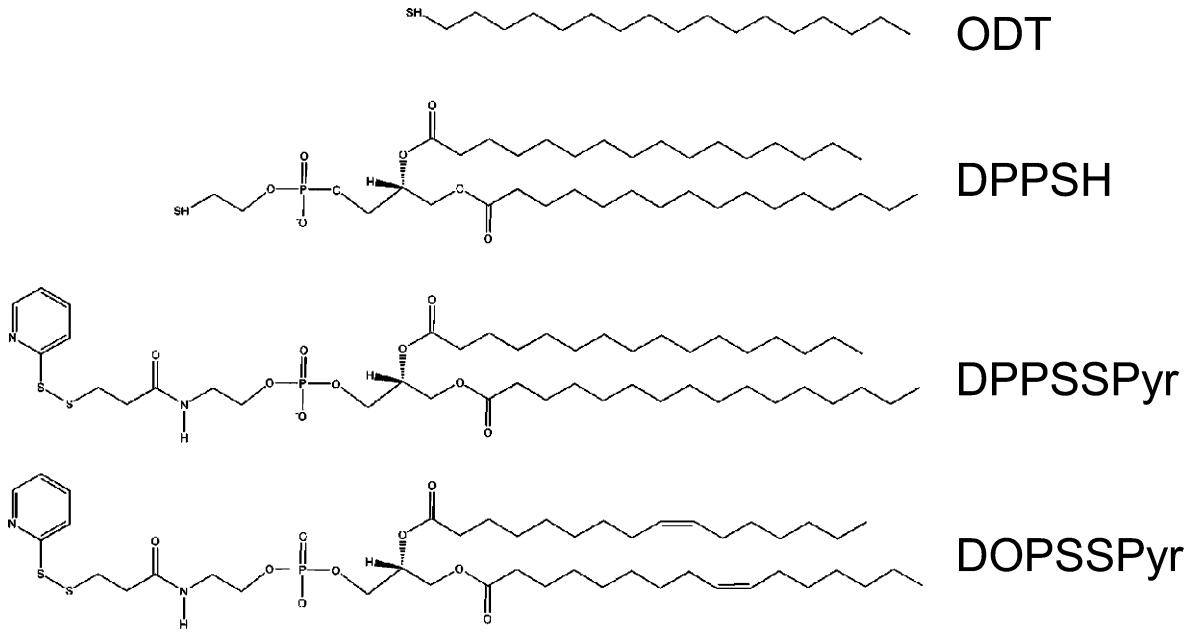

Figure 3. Chemical structures of the ODT, DPPSH, DPPSSPyr, and DOPSSPyr molecules used to make SAMs for HBMs.

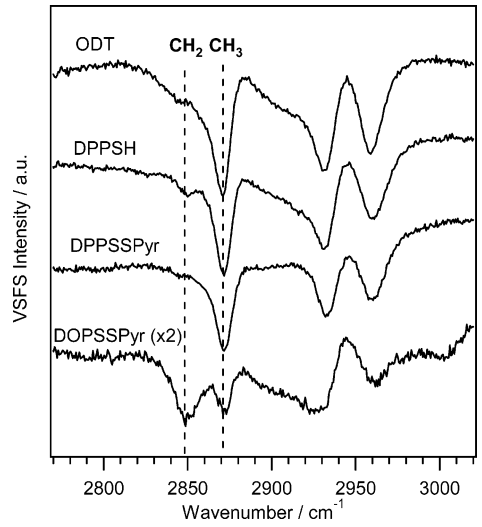

Figure 4. VSFS spectra in the C−H stretch region for HBMs composed of protonated SAMs of ODT, DPPSH, DPPSSPyr, and DOPSSPyr with a lipid overlayer of d62-DPPC taken at room temperature (T = 23 °C).

normalized d^+/r^+ amplitude ratios for d62-DPPC and d54-DMPC lipid monolayers on all SAMs are shown in Figure 5a and b, respectively. The values for T_m determined for both lipid outerlayers are summarized in Table 1. The error bars represent one standard deviation based on the pooled variance of all measurements. In general, HBMs made with DPPSH and ODT SAMs behaved similarly, raising T_m of the lipid layer substantially (from 7 to 15 °C) over T_m for corresponding vesicles. These SAMs have a very similar nature of the underlying alkane structure, that is, dense, well ordered, all-trans chains. HBMs of mixed SAMs using the disulfide molecules exhibit different behavior. HBMs formed on mixed SAMs of DOPSSPyr generally produced T_m the same as or just below that measured for lipids in vesicles. HBMs formed on DPPSSPyr exhibit intermediate behavior. In the case of d54-DMPC, T_m remains high (12 °C above vesicles) similar to that measured on DPPSH and ODT SAMs; however, for d62-DPPC/DPPSSPyr, T_m is similar to that on DOPSSPyr and of vesicles.

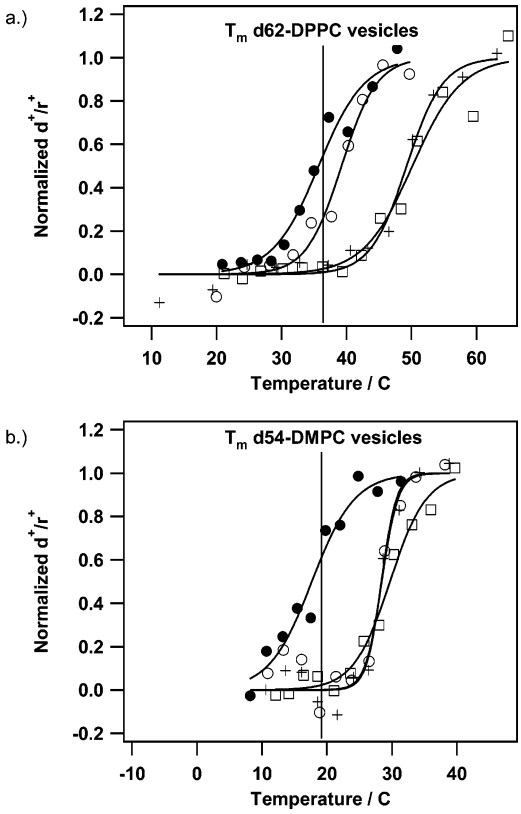

Figure 5. Representative normalized ratios of the d^+/r^+ amplitudes for HBMs composed of SAMs of ODT (+), DPPSH (□), DPPSSPyr (○), and DOPSSPyr(●) each with (a) a d62-DPPC lipid overlayer and (b) a d54-DMPC lipid overlayer. The corresponding vertical lines are T_m for d62-DPPC or d54-DMPC vesicles in solution.

All of the HBMs measured in this study have transition widths (taken from the full width at half-maximum of the derivative of the sigmoid fits) that range from 8 to 17 °C, presented in Table 1. These widths are significantly broader than the ≤1 °C widths reported by DSC thermograms or IR frequency shifts for large unilamellar or multilamellar vesicles.[41] The transition

widths are also broader than what we have previously reported for a similar system, protonated lipids on dODT (4−7 °C).[22] We had previously ascribed the broader transition widths to a decrease in cooperativity between the lipid molecules in the HBM or due to a reduced cooperative unit size often observed for these systems.[50] In the transition widths reported here, there appears to be no trend related to the different underlying SAM surfaces, although it does appear that the d62-DPPC lipid layers have a narrower distribution of transition widths than do the d54-DMPC layers.

Previous measurements of T_m of lipid SPBs on glass or silica,[51−53] on mica,[10−12,54] and of lipid monolayers on hydrophobic silanized surfaces[55,56] provide insight into the possible mechanisms of lipid interactions within the SPBs. For PC lipid bilayers fused to planar glass substrates[51,53] or on silica beads,[52] T_m is reported to be at nearly the same temperature as unsupported PCs in vesicles as there is little interaction (i.e., uncoupling) between the glass substrate and the headgroups of the supported PC bilayers. More complex phase behavior has been reported for PC bilayers supported on mica substrates. DSC and ^{2}H NMR experiments for DPPC and D(C_{15})PC multilayers on high surface area mica chips[10] revealed several phase transitions: one at T_m similar to vesicles, and two at $T_m + 2$ °C and $T_m + 4$ °C higher than vesicles. The lowest T_m was attributed to the multilayer, the next higher T_m to the top leaflet of the mica-bound bilayer, and the highest T_m to the lower leaflet closest to the mica. This result was more recently confirmed for bilayers on mica with AFM.[11,12,54] It has been proposed that an electrostatic interaction between the headgroup of the lower lipid leaflet with the mica surface increases T_m for that layer and also propagates weakly to an increase in T_m for the second layer (top leaflet of the mica-bound layer). Thus, the phase transitions in the two lipid leaflets are decoupled.

Similar to the HBM systems presented in this paper, T_m has been determined by DSC and ^{2}H NMR for d62-DPPC monolayers on C18 silanized spherical glass beads[55] and has been reported to be 8.6 °C higher than d62-DPPC multilamellar vesicles. This is a decoupled phase transition between a lipid monolayer and a solid support because the silanized layer on the support remains in its crystalline state and does not undergo a phase transition concurrent with the lipid transition. In a publication involving HBMs of protonated lipids on similarly silanized silica,[56] a trend in T_m for PC lipids ranging from 1,2-dilauroyl-*sn*-glycero-3-phosphocholine, DLPC (C12), to 1,2-diarachidoyl-*sn*-glycero-3-phosphocholine, DAPC (C20), was observed. For HBMs on C18-silanized silica, T_m was reported to be 18.1 °C higher for DLPC, 11.2 °C higher for DMPC, 5.6 °C higher for DPPC, 1.3 °C lower for 1,2-distearoyl-*sn*-glycero-3-phosphocholine, DSPC (C18), and 8.6 °C lower for DAPC relative to T_m for the respective large lipid vesicles in solution. This trend was attributed by the authors to an interdigitized packing of the lipids (in the gel phase) into the hydrophobic silane layer with optimized packing for equal chain lengths, that is, for DSPC (C18) in C18-silanized chains. Interdigitization may be possible for silanized layers on silica due to the decreased packing density of the C18-silane chains on silica,[57] which has been shown to depend on the pretreatment of the silica surface with hydroxyl or water moieties.

As just presented, the nature of the support affects the phase transition temperature of SPBs and the lipid layer in HBMs. In a previous publication,[22] we reported an increase of about 10 °C for T_m of the lipid layer relative to the corresponding T_m of vesicles in solution for HBMs made from DMPC and DPPC on dODT/Au SAMs. In the current experiments, we also observe similar increases in the transition temperatures of HBMs composed of d54-DMPC and d62-DPPC on both ODT and DPPSH SAMs relative to the T_m of the respective lipids in vesicles. It is clear that the dominant physical interactions in the HBMs comprised of lipids on dense alkane SAMs are different from those proposed for either SPBs on mica or lipid monolayers on silanized silica. We can eliminate the possibility of electrostatic attraction of the lipid to the SAM covered Au surface because electrically neutral SAMs on uncharged Au were used. We can also eliminate simple interdigitation of the lipid layer into the SAM because of the higher packing density of alkane chains of ODT and DPPSH molecules in the SAM (as compared to C18-silane), which keeps the SAM crystalline and impenetrable at all temperatures investigated in this study (<65 °C), consistent with previous studies of the melting temperature of related alkanethiolate systems.[58−60] Thus, the mechanism for the increased T_m in our lipid/dODT and lipid/DPPSH HBMs is therefore different from mechanisms proposed for related SPBs. We proposed a possible explanation for the increased T_m and broadened transition width of alkanethiolate HBMs: the hydrophobic interaction of the lipid tails with the dODT surface could effectively confine the lipids, inhibiting the lateral expansion of the lipid layer and thus raising T_m in HBMs relative to vesicles. Lipid confinement could also lead to a smaller cooperative unit size undergoing the melting transition, consistent with a broadened transition width.

The varying results for the HBMs on the mixed pyridine disulfide SAMs suggest that the critical lipid/SAM interactions are complex. For the mixed SAMs, we envision the surface composed of the lipid thiolate (DPPS- or DOPS-) and pyridine thiolate (PyrS-). The DOPSSPyr SAM presents an alkane surface to the upper leaflet that differs from that of ODT and DPPSH in two aspects: the total chain density is presumably lower, and the chain conformation is disordered as evidenced in the VSFS spectra presented in Figure 4. For both HBMs formed on this disordered SAM, T_m is essentially equal to that observed in vesicles. This result suggests that, unlike the cases of ODT and DPPSH HBMs, there is little or no confinement of the lipid tails at the DOPSSPyr SAM interface, thus allowing the lipids to have a lower transition temperature.

We observe a disparity in phase behavior of the different lipid overlayers in HBMs formed on the DPPSSPyr surface. In the

(50) Tokumasu, F.; Jin, A. J.; Dvorak, J. A. *J. Electron Microsc.* **2002**, *51*, 1−9.
(51) Liu, J.; Conboy, J. C. *J. Am. Chem. Soc.* **2004**, *126*, 8894−8895.
(52) Naumann, C.; Brumm, T.; Bayerl, T. M. *Biophys. J.* **1992**, *63*, 1314−1319.
(53) Lee, C.; Bain, C. D. *Biochim. Biophys. Acta* **2005**, *1711*, 59−71.
(54) Keller, D.; Larsen, N. B.; Moller, I. M.; Mouritsen, O. G. *Phys. Rev. Lett.* **2005**, *94*, 025701-1−025701-4.
(55) Linseisen, F. M.; Hetzer, M.; Brumm, T.; Bayerl, T. M. *Biophys. J.* **1997**, *72*, 1659−1667.
(56) Käsbauer, M.; Bayerl, T. M. *Langmuir* **1999**, *15*, 2431−2434.
(57) Wang, R.; Guo, J.; Baran, G.; Wunder, S. L. *Langmuir* **2000**, *16*, 568−576.
(58) Schreiber, F.; Eberhardt, A.; Leung, T. Y. B.; Schwartz, P.; Wetterer, S. M.; Lavrich, D. J.; Berman, L.; Fenter, P.; Eisenberger, P.; Scoles, G. *Phys. Rev. B* **1998**, *57*, 12476−12481.
(59) Bansebaa, F.; Ellis, T. H.; Badia, A.; Lennox, R. B. *J. Vac. Sci. Technol., A* **1995**, *13*, 1331−1336.
(60) Schreiber, F.; Gerstenberg, M. C.; Dosch, H.; Scoles, G. *Langmuir* **2003**, *19*, 10004−10006.

case of a d54-DMPC HBM, T_m is 11.6 °C higher than T_m for vesicles, that is, in the same range as that previously observed for d54-DMPC on the other crystalline SAMs, despite the possible packing density difference on this mixed SAM surface. However, when an HBM is made on this mixed SAM with d62-DPPC, T_m is observed only 1.3 °C higher than T_m for vesicles. Thus, it appears that d62-DPPC is interacting differently with the DPPSSPyr SAM as compared to d54-DMPC. While the VSFS spectrum of this SAM (presented in Figure 4) appears to still be crystalline (similar to the DPPSH and ODT spectra), the presence of the coadsorbed PyrS- may lower the lipid density and/or introduce underlayer defects that impart a level of conformational flexibility to the interface that is lacking in the ODT and DPPSH SAMs.

The striking contrast of lipid T_m between the dense packed HBMs on ODT and DPPSH and the HBMs on the disordered DOPSSPyr, and the disparity of lipid behavior in the DPPSSPyr system, seems to indicate that specific intermonolayer interactions are important. As discussed previously, Käsbauer and Bayerl[56] observed a trend in T_m for similar HBMs of PC lipids on C18-silanized silica. This trend was attributed by the authors to an interdigitated packing of the lipids in the gel phase into the hydrophobic silane layer with optimized packing for chains of equal lengths, that is, for DSPC (an 18-carbon chain) into C18-silanized chains, giving T_m for the DSPC lipids very close to that observed in vesicles. We propose that this explanation does not apply to our HBMs. In the case of ODT and DPPSH HBMs, no interdigitation is possible due to the high packing density of the alkane chains in the SAM. In the case of the mixed SAMs, full interdigitation is unlikely; however, partial interdigitation of the lipid into the SAM may be possible. In studies of asymmetric mixed-chain PC vesicles, partial interdigitation can lower T_m by ~10 °C relative to symmetric lipid vesicles.[61] The interaction of the lipids with the range of SAMs used in this study may also cause the gel-phase packing density of the lipid to be altered from that found in vesicles. If the underlying SAM influences or confines the packing of the alkane tails at the intermonolayer interface in the gel phase to be more closely packed than in a gel-phase vesicle, the headgroups would also be more closely packed and consequently less hydrated. T_m has been shown to be increased when the hydration of the headgroups is decreased.[62] Perhaps this is the case for HBMs formed on the crystalline SAMs, ODT, and DPPSH. In the extreme case of the DOPSSPyr HBMs, we proposed little interaction of the lipid layers with the SAM. The lipids in these HBMs may adopt a more natural gel-phase packing density similar to vesicles, and consequently have T_m values similar to those of vesicles. The intermediate case of the DPPSSPyr SAMs, where different length lipids have differing behavior, is difficult to explain and suggests that intermonolayer interactions are complex and require significant theoretical consideration in the future.

Conclusions

VSFS has been used to determine the lipid phase transition temperature in HBMs. We have demonstrated for two different chain length lipids (DMPC and DPPC) that the phase transition temperature varies with the packing density and crystallinity of the underlying SAM. We expect that selection of other SAMs or the design of mixed SAMs between the disordered DOPSSPyr and the crystalline ODT will permit tuning of T_m throughout the intermediate values. The sensitive dependence of the supported lipid T_m on the nature of the underlying SAM may lead to new insights regarding the nature of inter-leaflet interactions on the phase behavior of lipid layers in general. The ability to tune the composition and properties of HBMs will enable their optimization as an environment for studying membrane proteins under physiological conditions and in well-defined orientations.

Acknowledgment. We gratefully acknowledge support from the intramural NIST Advanced Technology Program. N.A.A. wishes to acknowledge the National Research Council for postdoctoral fellowship support. J.C.S. is contracted by NIST and is officially an employee of KT Consulting, Inc.

JA066588C

(61) Chen, L.; Johnson, M. L.; Biltonen, R. L. *Biophys. J.* **2001**, *80*, 254−270.

(62) Wolfe, J.; Bryant, G. *Cryobiology* **1999**, *39*, 103−129.